A 4-decade record of elevation change of the Amery Ice Shelf, East Antarctica

M. A. King, R. Coleman, A. J. Freemantle, H. A. Fricker, R. S. Hurd, B. Legresy, L. Padman, R. Warner

A 4-decade record of elevation change of the Amery Ice Shelf, East Antarctica

Matt A. King,[1] Richard Coleman,[2,3,4] Anna-Jane Freemantle,[1] Helen Amanda Fricker,[5] Rachael S. Hurd,[6] Benoit Legrésy,[7] Laurie Padman,[8] and Roland Warner[9,3]

Received 24 June 2008; revised 17 October 2008; accepted 13 November 2008; published 30 January 2009.

[1] We report on long-term surface elevation changes of the central Amery Ice Shelf (AIS) by comparing elevation records spanning 4 decades (1968–2007). We use elevation records acquired with the following methods: optical leveling (1968–1969); ERS radar altimetry (1992–2003); GPS (1995–2006); and Ice, Cloud, and land Elevation Satellite (ICESat) laser altimetry (2003–2007). We compute multidecadal elevation trend (dh/dt) values at crossovers between the leveling route and each of the GPS and ICESat tracks as well as shorter-period dh/dt at ERS-ERS, GPS-GPS, and ICESat-ICESat crossovers. At GPS-leveling crossovers the mean long-term dh/dt is -0.003 m a^{-1}, and at ICESat-leveling crossovers the mean dh/dt is $+0.013$ m a^{-1}; neither trend is significantly different from zero. The data do, however, exhibit variable trends: near-zero change between 1991 and mid-1996, then thickening to ~2003, followed by thinning ~2003–2007, with 5 year dh/dt averages exceeding ~$\pm$0.1 m a^{-1}. The changes in dh/dt pattern in mid-1996 and again in 2003 occur with unexpected speed. The ice shelf exhibits different dh/dt patterns than does the surrounding grounded ice, suggesting that surface mass balance variations or longer-term variations in firn densification processes are unlikely to be major causes. We conclude that these observed multiyear elevation changes must be due to currently unexplained or presently poorly quantified phenomena involving surface or basal processes and/or ice dynamics. With the multidecadal stability of the AIS established, the short-term fluctuations that we observe suggests that for other ice shelves, observed strong dh/dt signals over short time periods do not necessarily indicate ice shelf instability.

Citation: King, M. A., R. Coleman, A.-J. Freemantle, H. A. Fricker, R. S. Hurd, B. Legrésy, L. Padman, and R. Warner (2009), A 4-decade record of elevation change of the Amery Ice Shelf, East Antarctica, *J. Geophys. Res.*, *114*, F01010, doi:10.1029/2008JF001094.

1. Introduction

[2] Disintegration of Antarctic ice shelves can result in accelerated outlet glacier flow [e.g., *Rignot et al.*, 2004] and, consequently, sea level rise. Ice shelf instability is likely related to changes in temperature of both the atmosphere and ocean [e.g., *Scambos et al.*, 2000; *Shepherd et al.*, 2003]. To monitor the health of an ice shelf, long time scale (decades) observations of surface elevations are required to separate short-term fluctuations from changes that may reflect secular trends. On shorter time scales (several years), elevation trends are subject to variations in environmental conditions; e.g., decadal variations in regional accumulation patterns could be as much as ~$\pm$25% of the long-term mean [*Monaghan et al.*, 2006]. It has recently been suggested that multidecadal variations in prior accumulation can have a complicated influence on current elevation changes via anomalies in the thickness of the firn layer [*Helsen et al.*, 2008].

[3] For Antarctica's ice shelves, continuous records of elevation change spanning several decades unfortunately are rare. The earliest geodetic quality leveling data on ice shelves were collected during the mid-to-late 1960s [e.g., *Dorrer et al.*, 1969], and accurate GPS measurements have only been available since the mid-1990s. Satellite altimetry provides the most practical way to monitor surface elevation change on ice shelves, but the most suitable altimeter data

[1]School of Civil Engineering and Geosciences, Newcastle University, Newcastle upon Tyne, UK.
[2]Centre for Marine Science, University of Tasmania, Hobart, Tasmania, Australia.
[3]Also at Antarctic Climate and Ecosystems CRC, Hobart, Tasmania, Australia.
[4]Also at CSIRO Marine and Atmospheric Research, Hobart, Tasmania, Australia.
[5]Institute of Geophysics and Planetary Physics, Scripps Institution of Oceanography, La Jolla, California, USA.
[6]Center for Spatial Information Science, University of Tasmania, Hobart, Tasmania, Australia.
[7]LEGOS, CNES, UPS, IRD, CNRS, Toulouse, France.
[8]Earth and Space Research, Corvallis, Oregon, USA.
[9]Australian Antarctic Division, Department of the Environment, Water, Heritage, and the Arts, Kingston, Tasmania, Australia.

0148-0227/09/2008JF001094

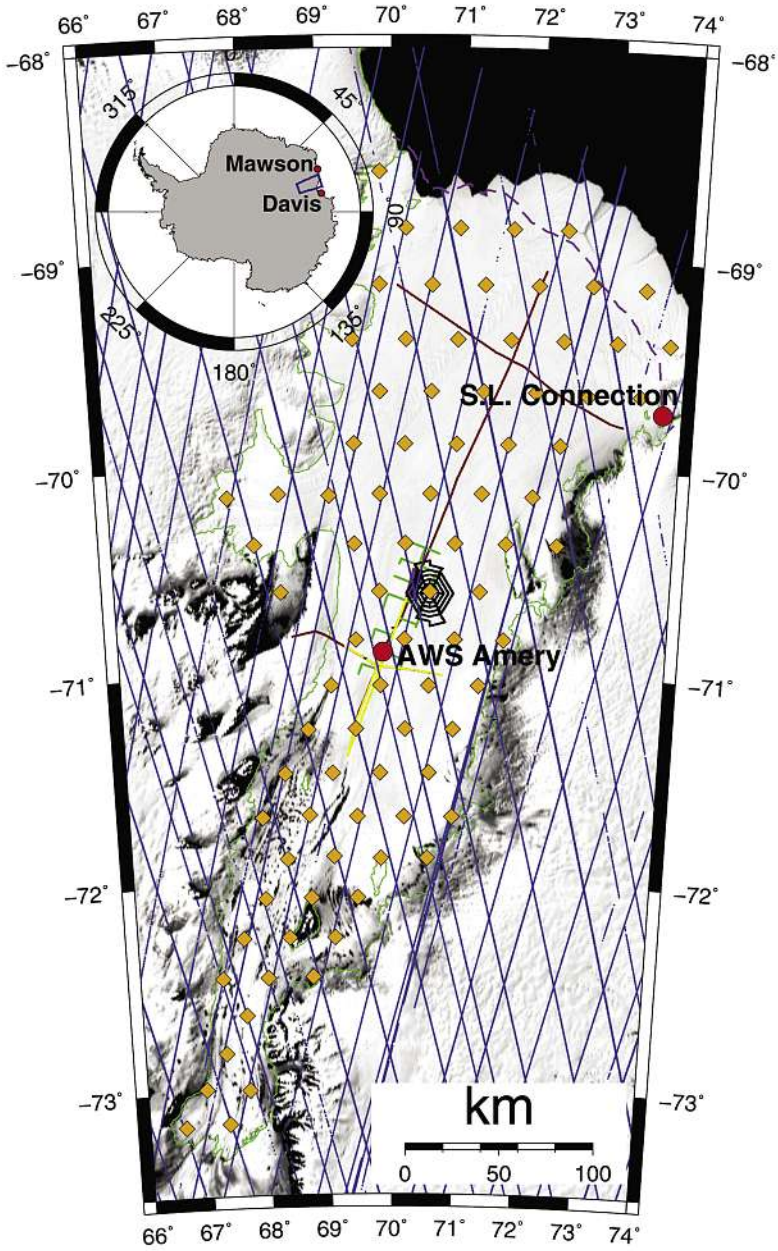

Figure 1. Overview of Amery Ice Shelf (AIS) surface elevation data sets used in this study, with the grounding line marked in light green. Data sets shown are the leveling route (dark red; only well-positioned portion shown), Ice, Cloud, and land Elevation Satellite (ICESat) ground tracks (blue), and kinematic GPS tracks (other colors). ERS-ERS crossover locations are shown as orange diamonds. Also shown are the locations of the automatic weather station and of the connection of the leveling to sea level. Note that the ice front has advanced considerably (~40 km) between the times of the leveling (late 1968; dashed purple line [*Fricker et al.*, 2002]) and the Mosaic of Antarctica (MOA) image acquisition (late 2003).

(from the Earth Remote Sensing (ERS)-1 and ERS-2 satellites) only extend back to 1992. *Zwally et al.* [2005], for example, used ERS Radar Altimetry (RA) to show that many Antarctic ice shelves increased or decreased in elevation with typical rates of ±(0.1–0.4) m a^{-1} over the period 1992–2001.

[4] The Amery Ice Shelf (AIS), East Antarctica (Figure 1), has a long record of elevation measurements, acquired using various methods between 1968 and 2007. The first geodetic quality optical leveling profiles were obtained in late 1968 in conjunction with observations used to generate precise velocity and strain data [*Budd et al.*, 1982; *King et al.*, 2007]. More than 500 km of the central AIS was surveyed along three profiles (two transverse and one longitudinal to the ice flow direction). Since 1995, GPS-derived elevation profiles have been obtained [e.g., *Phillips*, 1998]. In addition to the ERS-1 and ERS-2 data, laser altimetry data from the Ice,

Cloud, and land Elevation Satellite (ICESat) are available since 2003 [*Schutz et al.*, 2005]. In this paper, we report on crossover analyses of elevation data from these four sources (leveling, ERS, GPS, and ICESat) to assess the magnitude of interdecadal and intradecadal elevation change and variability of the central AIS. These comparisons represent one of the longest records of Antarctic ice shelf surface elevation data yet exploited.

2. Data Sets and Data Processing

2.1. Compatibility Issues for Ice Shelf Height Data

2.1.1. Reference Systems and Frames

[5] The fundamental data type used in this paper is observations of ice shelf surface height. One of the challenges in comparing heights from different sources is converting all data into the same geodetic reference system. Most notably, heights obtained from historic optical leveling require conversion from an instantaneous sea level datum to ellipsoidal heights before they can be compared to ellipsoidal heights collected by satellite-based technologies (e.g., GPS, altimetry). This conversion requires, among other corrections, an accurate model of the geoid-ellipsoid separation (typically referred to as a "geoid model") which has only recently become available for Antarctica through analyses of the data from the Gravity Recovery and Climate Experiment (GRACE) satellite mission. Errors in preGRACE global geoid models over the AIS region are up to ±3 m, due to lack of gravity observations in the region; the GRACE data have improved this by an order of magnitude. We use a recent (April 2008) GRACE-based static geoid model (EIGEN-GL04C; http://icgem.gfz-potsdam.de/ICGEM/ICGEM.html), calculated for the WGS-84 ellipsoid.

[6] Care must also be taken in adopting the same permanent solid earth tide convention. Altimetric height time series (including ERS and ICESat) are produced in a mean tide system, whereas GPS time series are currently produced in a conventional tide-free system [*McCarthy and Petit*, 2004]. The difference between the two is ∼0.10 m at the latitude of the AIS (the conventional tide-free surface being above the mean tide surface at this latitude). Throughout this paper we adopt a mean tide system; that is, we block shift the GPS time series by −0.10 m and compute geoid-ellipsoid separations in this system. The time-variable component of the solid earth tide has been modeled throughout with negligible residual error. After applying the abovementioned corrections (geoid, solid earth/mean tide), the leveling elevations are reduced to a system consistent with the International Terrestrial Reference Frame 2000 (ITRF2000) [*Altamimi et al.*, 2002].

[7] In addition to these corrections, comparison of heights from various sources relies on consistency in the reference frames used for each measurement type. Our GPS and ICESat elevations are produced in the ITRF2000. The ERS elevations described below are in a reference frame consistent with ITRF2000, at least at the level of a few mm a^{-1}, and we regard the difference as being negligible over the observation period of ERS.

[8] The ICESat elevations (release 428) are provided on the TOPEX/Poseidon ellipsoid, which we convert to the WGS-84 ellipsoid to be compatible with the GPS and leveling data.

2.1.2. Tide and Inverse Barometer Corrections

[9] Another challenge in comparing elevations over floating ice shelves is to correct all the data sources for the effects of ocean tides and atmospheric pressure variability (the "inverse barometer effect," IBE). Contributions from the tide and IBE can be significant in this region, being >1 m for the tide and up to ∼0.5 m for IBE. Tide errors directly affect GPS and altimetry measurements, and hence accurate corrections are required. In this paper, tidal corrections were made using the TPXO6.2 tide model [*Egbert and Erofeeva*, 2002], the most accurate global tide model currently available for this region [*King and Padman*, 2005], or a new AIS 2 km tide model, depending on the data set. The new 2 km model has a significantly more accurate and higher-resolution representation of the ice shelf margins (ice front and grounding line) of the AIS. For the purposes of the present study, the differences in tide predictions between this 2 km AIS model and TPXO6.2 are negligible. The ocean tide loading displacement was modeled also using TPXO6.2. The IBE was estimated from atmospheric pressure records from various sources according to the individual data set, as described below. The typical value of the IBE is ∼−0.01 m change in sea surface height per +1 hPa change in air pressure [*Padman et al.*, 2003].

2.2. Leveling (1968)

[10] The optical leveling route was surveyed during October–December 1968 (Figure 1) [*Budd et al.*, 1982]. Leveling heights (H) were obtained relative to instantaneous sea level (SL) on 30 December 1968. We recently returned to the archived field notes and reanalyzed the leveling observations. Unfortunately the exact time, t, of the SL connection was not found in the surviving field notes. Personal diary entries (M. Corry, unpublished diary, 1968–1969) state that the SL connection was made during "mid late afternoon" local time (local time is GMT+6 h); so we set t to 1200 UT. Conversion of H to ellipsoidal heights (h) is given by

$$h = H - \eta_t - IBE_t + DOT + N + \varepsilon, \tag{1}$$

where η_t is the instantaneous tide height; IBE_t is the inverse barometer effect due to variations in atmospheric pressure (P); DOT is the mean dynamic ocean topography (height of the mean ocean surface above the geoid); and N is the geoid-ellipsoid separation, evaluated at each leveling location. The first three correction terms are evaluated at the SL connection location. We take DOT and N to be time-invariant, with little error over the time periods considered. Residual errors (ε) are discussed below.

[11] Average measurement spacing along the leveling route is ∼150 m and locations for reference poles every 3–10 km along route are taken from *King et al.* [2007]. The locations of intermediate points were determined using "stadia tacheometry" (the process of measuring horizontal distances using an optical level; see *Schofield* [1993] for a complete description) with positional errors less than ∼10 m on average. Random errors in leveled height differences accumulate at the end points of the leveling lines (relative to the northeast AIS) and reach ∼0.2 m over the length of the lines, with mean values of 0.15 m.

[12] We applied tide corrections using the TPXO6.2 tide model [*Egbert and Erofeeva*, 2002]. The timing uncertainty

at time t will introduce an error into the tide correction, but this is small, since the connection occurred during a turning diurnal tide, so the maximum error is only ~0.2 m, contributing less than 0.01 m a^{-1} to uncertainty of long-term (30 year) estimates of rates of elevation change for a given geographical location (dh/dt). For the IBE_t correction, P values are not available for the date and location of the SL connection. Over our study region, mean pressure values have changed slightly between 1968 and 2007 [*Heil*, 2006] and neglecting IBE would fail to remove the small resulting dh/dt. We estimated an IBE_t value [*Padman et al.*, 2003] using pressure data recorded at Mawson Station (Figure 1). Mawson pressure was first corrected to an AIS mean surface pressure (981.2 hPa) using data from an automatic weather station (AWS) deployed at G3 in the central AIS (Figure 1) during 1999–2003. Comparison of 1999–2003 Mawson daily mean pressure with pressure from the G3 AWS showed a high correlation (r = 0.72) and no phase lag. Residual root-mean-square (RMS) between Mawson and G3 values was 8.4 hPa (~0.08 m IBE) and hence we assigned this error for IBE_t. We thus consider the error in IBE due to the timing error to be negligible.

[13] We obtained geoid-ellipsoid separation (N) values (equation (1)) at each leveling location from EIGEN-GL04C. The lack of gravity data in this region makes it difficult to make accurate local error estimates for N, but it is ~0.3 m globally based on a global GPS/leveling comparisons [*Förste et al.*, 2008]. Larger errors have been found in EIGEN-GL04C over grounded ice in the Southern Prince Charles Mountains/Lambert Glacier basin upstream of the AIS [*Scheinert et al.*, 2008], at higher spatial scales than those sampled by EIGEN-GL04C, but those results are in an area of large topographic variation unlike our study area. We consequently adopt 0.3 m as our error estimate for N.

[14] Mean DOT values (as appearing in the right hand side of equation (1)) were obtained from a specially provided (D. Chambers, personal communication, 2006) unsmoothed version of the *Chambers* [2006] model extended to the Antarctic coastline. These values were then smoothed over 400 km (half wavelength) to overcome GRACE-related errors. Seasonal deviations from the mean DOT are small in this region. Evaluation of the DOT model at the leveling connection site gave a value of −1.5 m. Errors are probably <0.05 m [*Chambers*, 2006]. There will also be some small residual deviation from this mean DOT but we regard this as negligible when computing dh/dt over 30-year time spans.

[15] We assessed the accuracy of the N and DOT corrections for this region at Davis Station (Figure 1) where h and H observations of mean sea level are available [*Watson*, 2005]. Differencing these observations gives values within 0.05 m of the sum of N and DOT, suggesting that the $N + DOT$ corrections applied to the AIS leveling elevations are likely accurate.

[16] For practical reasons, the 1968 surveyors performed the leveling at points of locally high elevation, which introduces a positive bias in those heights. When comparing these heights with heights derived from GPS and ICESat with their different (effectively random) sampling geometries, this will introduce a negative bias in the estimated dh/dt. On the basis of kinematic GPS profiles on the central AIS, elevation changes over distances of 150 m can typically be up to 1 m, giving an upper bound of this bias of ~−0.03 m a^{-1} when considering the time period between the leveling and other data sources. However, Monte Carlo simulations of height profiles moving at speeds of the ice shelf motion suggest that the likely magnitude of a 30-year dh/dt bias is no more than ~−0.01 m a^{-1}.

2.3. GPS Surveys (1995–2006)

[17] Kinematic GPS surveys of the ice shelf surface along profiles were carried out in 1995, 1999, 2001, 2003, and 2006 using snowmobiles. Surface elevation was sampled every 10–30 s which, given the speed of snowmobile travel, is equivalent to a point every 30–90 m. We processed data from all of these campaigns using the *Track* kinematic GPS software [*Chen*, 1998; *King and Bock*, 2006], relative to a local ice shelf base station whose coordinates were determined using kinematic precise point positioning (PPP) [*King and Aoki*, 2003]. Ocean tide loading displacements were modeled in the PPP analysis. The exception to this analysis procedure was the 1995 data where we simply adopted the analysis described by *Phillips* [1998]. Tidal corrections were made to each GPS data set using TPXO6.2. IBE corrections were made using data from the AWS (after 1999) or using corrected Mawson data (1995 and 1999). We produced the GPS elevations on the WGS-84 ellipsoid and applied the correction for the permanent tide. Uncertainties of the GPS-derived heights are ~0.05 m with effectively zero bias.

[18] We computed elevation change rates at GPS-GPS crossovers (that is, crossovers between two different GPS profiles) using the Akima spline interpolation technique [*Wessel and Smith*, 1998]. We used six elevations either side of the crossover in the interpolation. Only crossovers for which $dt > 2.5$ years were analyzed to ensure robust dh/dt estimates in the presence of seasonal signals [*Blewitt and Lavallée*, 2002]. No outliers needed to be removed from this data set.

2.4. ERS-1 and ERS-2 Data (1992–2003)

[19] We obtained radar altimeter data, acquired by the ERS-1 and ERS-2 satellites, from http://icesat4.gsfc.nasa.gov/index.html, as Level 2 ice data records (version 5), covering the period 1992–2003. These data have the NASA/GSFC V5 range-retracking algorithm, atmospheric range corrections, instrument corrections, slope corrections and an adjustment for solid earth tides applied [*Zwally and Brenner*, 2001; *Zwally et al.*, 2005]. We only used data from the 35-day repeat phases (Phases C and G of ERS-1; all of ERS-2), and we used a mixture of ocean and ice mode data. NASA/GSFC applied instrument corrections include: removal of a 40.9 cm bias from ERS-1 elevations to account for a change in instrument parameter used for ERS-2 [*Femenias*, 1996]; corrections for drifts in the ultrastable oscillator and bias changes in the scanning point target response that are obtained from ESA; and upgraded orbits (DGM-E04 orbits) which have a radial orbit precision of 5–6 cm [*Scharroo and Visser*, 1998].

[20] The ocean tides modeled in the NASA/GSFC processing chain were added back in (since the implemented CSR3 tide model is not accurate in Antarctica) [*King and Padman*, 2005; *King et al.*, 2005]; we derived better tide corrections using the 2 km tide model and applied these to the

ERS heights. We modeled ocean tide loading displacements based on TPXO6.2. We estimated the IBE corrections using surface pressure data from NCEP Reanalysis model output [*Kalnay et al.*, 1996] by extracting a record for a point on the center of the AIS (70°E, 70°S) and then computing the IBE correction relative to the same mean pressure used for the other data sets. Since pressure systems have large spatial scales, this procedure will remove the majority of the IBE effect.

[21] We used crossover analysis to produce *dh*/*dt* estimates at ERS orbital crossover locations. ERS satellite ground tracks only repeat to ±1 km from the reference track, and to avoid problems with cross-track topography we excluded elevation measurements further than 1 km from a nominal (median) crossover location from the *dh*/*dt* calculation. We also removed individual crossover points located within 10 km of the grounding zone. Further filtering was done by excluding crossovers in the following three cases: (1) <50 samples; (2) dt < 5 years; or (3) detrended time series with standard deviations >2 m. For the remaining crossovers, *dh*/*dt* and its uncertainty, $\sigma_{dh/dt}$, were computed assuming a linear plus annual cycle model with the initially uniform variance-covariance matrix of the model parameters scaled to unit a posteriori variance. These *dh*/*dt* values were then smoothed using all $(dh/dt)_i$ (where i denotes an individual crossover *dh*/*dt*) estimates within a distance l (in km), such that l_i < 50 km from each ith crossover location, using an inverse distance weighting scheme:

$$dh/dt_{smooth} = \frac{\sum_{i=1}^{n} \left\{ (dh/dt)_i \cdot \left(\sigma_{i,dh/dt}^2 + (l_i/200)^2 \right)^{-1} \right\}}{\sum_{i=1}^{n} \left(\sigma_{i,dh/dt}^2 + (l_i/200)^2 \right)^{-1}}$$

The second term in the weighting factor down weights a point at 50 km, with typical $\sigma_{dh/dt}$ of ∼0.1 m a^{-1}, by an additional 0.25 m a^{-1} (in quadrature). Alternative weighting schemes could be applied, but this one preserves local features while reducing noise sufficiently well for our purposes.

[22] We did not correct for the effects of glacial isostatic adjustment on the grounded ice sheet since the effect in this region is likely small (<±2 mm a^{-1}) and uncertain [e.g., *Ivins and James*, 2005]. The effects of firn densification on ERS, and our other elevation measurements, are discussed later.

2.5. ICESat Data (2003–2007)

[23] We used ICESat laser altimeter data for the period October 2003 to April 2007 from the following ICESat campaigns: Laser 2a, 2b, 3b, 3c, 3d, 3e, 3f, 3g, and 3h. Data from these campaigns are all available as Release 428, which are fully calibrated and include final orbit and attitude corrections. We used geolocated ICESat footprint locations, ocean tide and ocean tide loading corrections, atmospheric pressure, and receiver energy and gain from the GLA12 data product. A low gain saturation correction was applied [*Fricker et al.*, 2005]. The elevations were converted to the WGS-84 ellipsoid and the tides from the ICESat processing chain added back in. Improved tide corrections were applied using TPXO6.2 (along-track data) or the AIS 2 km tide model (crossover data). In both cases ocean tide loading displacements were modeled on the basis of TPXO6.2. The IBE was corrected using surface atmospheric pressures supplied with the ICESat records. In ideal conditions, ICESat Laser 2a elevations are biased too low by <0.02 m (too high by <0.02 m after correction for the permanent tide) with an uncertainty of <0.03 m [*Fricker et al.*, 2005]. Over rougher surfaces, biases per satellite pass may increase substantially, although the mean bias remains close to zero [*Shuman et al.*, 2006]. Intercampaign elevation biases are present in ICESat data, but these are of order 0.1 m and are somewhat random in time. In our subsequent analysis, we used an uncertainty of 0.1 m for each ICESat elevation measurement.

[24] We used along-track ICESat data in the comparison with the leveling data. We also computed values of *dh*/*dt* at ICESat-ICESat crossovers for analysis of shorter-term elevation changes. ICESat ground tracks are not exactly repeated (±200 m deviation from a reference track) and we merged (in a least squares sense, with no distance-dependent down weighting) *dh*/*dt* estimates within 5 km of each nominal crossover location to obtain one crossover per 5 km at maximum. For the ICESat-ICESat comparison we removed crossovers for which (1) dt < 2.5 years; (2) $|dh/dt|$ > 0.5 m a^{-1}; or (3) uncertainties > 0.05 m a^{-1}. Only a small number of *dh*/*dt* values were large, and at least some of these appeared to be related to surface crevasses visible in satellite imagery.

3. Results

3.1. Elevation Change Rates Over 30–40 Years

[25] We computed values of *dh*/*dt* at GPS-leveling and ICESat-leveling crossovers in the same manner as for the *dh*/*dt* values at GPS-GPS crossovers (section 2.2). We did not directly compare elevations derived from RA to those from the other techniques since the RA has a large footprint (2–3 km over ice) and measures to a different surface. In addition, *Thomas et al.* [2008] report that ERS-derived *dh*/*dt* for Greenland may exceed measurements of actual surface *dh*/*dt* by several cm a^{-1}, probably due to a progressive lifting of the radar-reflecting horizon within the upper snow layer. They suggested year-on-year increases in summer melting in Greenland, and consequent changes in near-surface snow properties, as one possible mechanism to explain the effect. The extent of any such differences for Antarctica remains to be established.

[26] We note that ICESat elevations represent an average over a footprint of ∼65 m in diameter, whereas the GPS and leveling heights are effectively point values. This will introduce some small elevation variation at crossover locations.

[27] The spatial distribution of *dh*/*dt* for the 203 multidecadal intertechnique records (84 GPS-leveling crossovers and 119 ICESat-leveling crossovers) is shown in Figure 2. The ICESat-leveling crossovers sparsely cover a larger region of the AIS, whereas the GPS-leveling crossovers are mainly concentrated in the central AIS region. Most of these crossover values show close to zero change over the periods considered (∼27–38 years and ∼39 years, respectively). The GPS- and ICESat-derived values show close agreement, suggesting any intertechnique bias is small. The ICESat-derived *dh*/*dt* (Figure 3) are normally distributed at the 5% significance level as determined in a Lilliefors test, while the GPS-derived values are not normally distributed. This may reflect

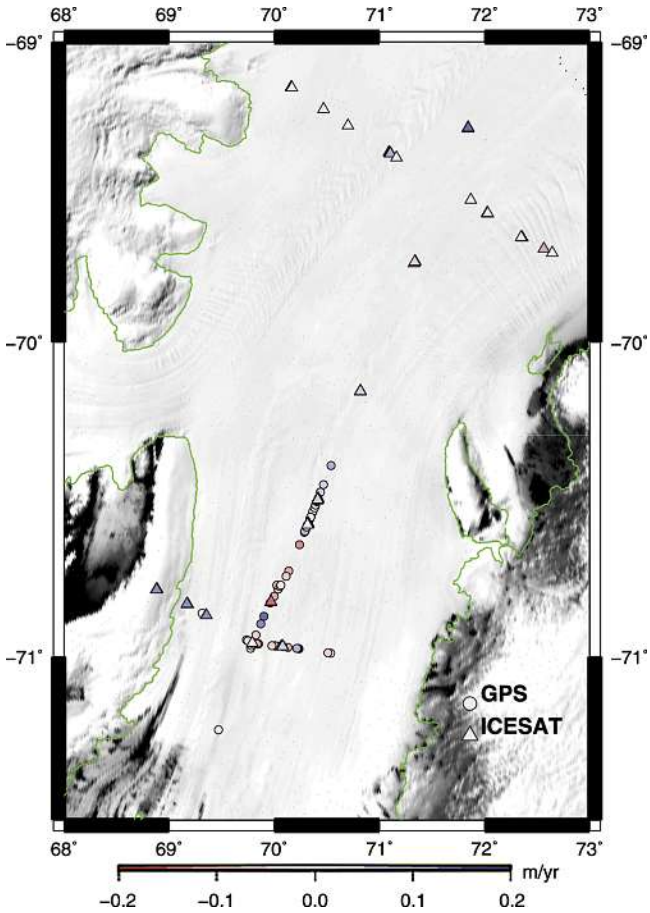

Figure 2. Derived *dh*/*dt* values from GPS-leveling (circles) and ICESat-leveling (triangles) crossover comparisons.

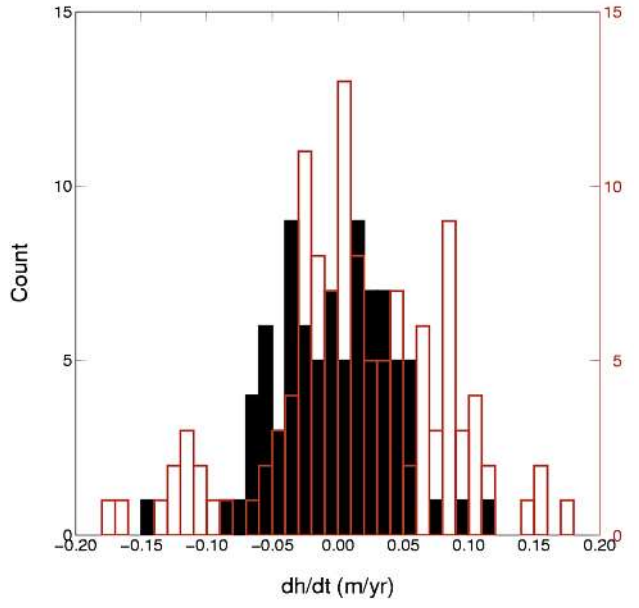

Figure 3. Histogram of *dh*/*dt* estimates on AIS for GPS-leveling (black) and ICESat-leveling (red) crossovers.

the small area sampled by the fewer GPS crossovers, with smaller-scale features playing a more dominant role in the sample. The histograms of *dh*/*dt* have standard deviations of 0.044 m a^{-1} (ICESat) and 0.068 m a^{-1} (GPS), respectively.

[28] Mean *dh*/*dt* values are −0.003 m a^{-1} for GPS and +0.013 m a^{-1} for ICESat (Figure 4). Estimated (one sigma) errors are 0.011 m a^{-1} and 0.009 m a^{-1}, respectively, on a point-by-point basis. These errors are highly correlated between crossover locations and hence data averaging does not substantially reduce the errors of the *dh*/*dt* estimate. Statistically, the *dh*/*dt* values do not differ from zero at the 95% confidence level.

[29] Accounting for potential systematic biases in the leveling data set (Section 2), the *dh*/*dt* for GPS minus leveling could range between −0.011 and +0.005 m a^{-1} and the *dh*/*dt* for ICESat minus leveling could range between +0.019 and +0.007 m a^{-1}; the errors stated above also apply. These ranges are dominated by the potential error in the leveling tidal correction (η_t in equation (1)) due to the uncertainty in timing the connection to sea level. Change in mean sea level (globally ∼+0.002 m a^{-1}) introduces a further bias into these *dh*/*dt* estimates, although we do not apply a correction since its rate of change for this region is unknown.

[30] Our mean ∼38-year *dh*/*dt* values do not agree with the value derived by *Zwally et al.* [2005] from ERS RA over the period 1992–2001. They reported +0.150 ± 0.017 m a^{-1}

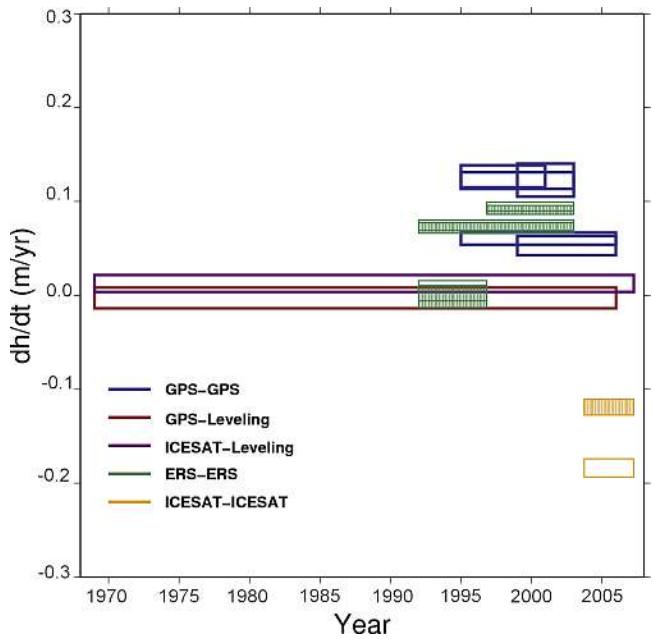

Figure 4. Mean *dh*/*dt* estimates derived at crossover locations on the AIS. Bar heights represent the 1σ errors of each height data set. Bar widths represent the time period over which the mean net *dh*/*dt* applies. The GPS-GPS crossover *dh*/*dt* are generated only from crossovers from epochs at each end of the bar, whereas all other *dh*/*dt* are generated from all available data. For ICESat and ERS crossovers, the unfilled polygons are for the region covered by the leveling and GPS, defined with a latitudinal cutoff at 72°S. The filled polygons are for all ERS and ICESat crossovers on the AIS.

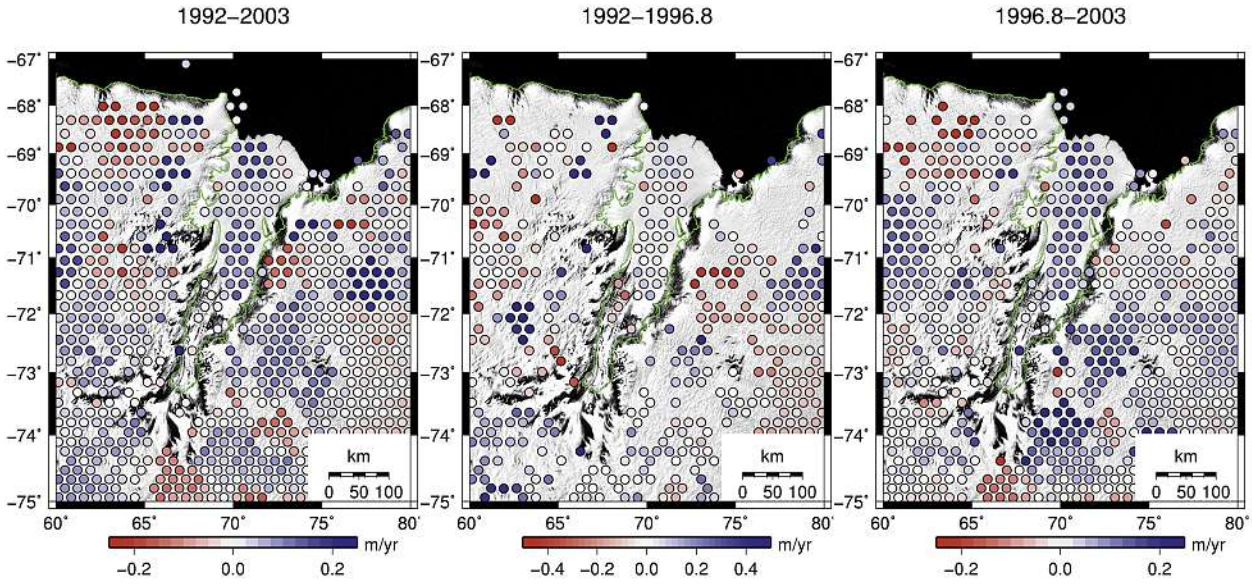

Figure 5. ERS-derived *dh*/*dt* at crossover locations for its (left) full observation period, (middle) period of low *dh*/*dt* on the AIS, and (right) period of positive *dh*/*dt* on the AIS. There are a few crossovers offshore on semipermanent sea ice, but these do not substantially affect our subsequent analyses.

from crossovers within a region of radius 100 km, centered on a crossover point in the northeast AIS. For the central and northern AIS, visual inspection of Figure 2b of their paper suggests a mean value closer to +0.10 m a^{-1}. The discrepancy suggests either an error in one or more of the leveling/GPS/ICESat/ERS data sets or substantial decadal level variations in AIS elevation, both positive and negative.

3.2. Intradecadal Elevation Change Rates

[31] To investigate the apparent discrepancy between our 1968–2007 results and those of *Zwally et al.* [2005] for 1992–2001, we increased our temporal sampling within the 1992–2007 period by using the ERS-ERS, GPS-GPS and ICESat-ICESat crossovers. This period has almost continuous observation from a combination of ERS and ICESat data. Elevation changes at the ERS crossovers for 1992–2003 are shown in Figure 5 (left). Considering only the values on the floating ice shelf, they suggest a net elevation increase at the ice front, with elevation decrease along the northeastern margin.

[32] To examine the ERS elevation time series, for each crossover location we combined all crossover time series within a search radius of 100 km of that point. This is complicated since each crossover series has a different mean height, different sampling epochs and, potentially, different *dh*/*dt*. The latter was avoided by first comparing each series visually. We then estimated offsets for a common epoch for each crossover series to be merged. This was done in a modified linear regression, estimating a single trend for all crossover series and one offset term per crossover series. The various time series were weighted uniformly. We then subtracted the respective offsets to produce a ''reconstructed'' merged time series.

[33] A typical combined elevation time series for one crossover location is shown in Figure 6. On the basis of significant peaks in the time series spectra, the main geophysical signal appears at one and two cycles per year with smaller amplitude signal at three and four cycles per year, in addition to the linear term. The best fitting model, based on these parameters, is also shown in Figure 6. This time series shows a mean *dh*/*dt* close to zero or slightly negative from 1992 until ~1996.8, at which time the *dh*/*dt* signal switched to positive through to the end of the time series in 2003. Subdividing the data set in these two subperiods (1992–1996.8 and 1996.8–2003) reveals that there is a spatial pattern of a shift from low *dh*/*dt* to strong positive *dh*/*dt* across the entire ice shelf (Figure 5 middle and right). For the first subperiod (1992–1996.8), elevation changes are typically in the range −0.1 to +0.1 m a^{-1}. In the second subperiod (1996.8–2003) elevation changes shift to ~+0.1 to +0.2 m a^{-1} across the entire northern and central AIS. The reduced number of crossover locations for the earlier subperiod when compared to the full period is due to a lack of data at some crossovers during each subperiod, resulting in data spans that are too short for reliably estimating *dh*/*dt*.

[34] We compared our ERS-ERS crossover results to the results of *Zwally et al.* [2005], in particular we compared their Figure 2b with our Figure 5. The same ERS data are used, although some important differences in postprocessing exist. First, we only use 35-day repeat data over the period 1992–2003 to derive *dh*/*dt* whereas *Zwally et al.* [2005] use all available data over the slightly shorter period 1992–2001. Second, we detide the ERS data using a more accurate tide model which reduces the effects of tidal aliasing. Third, we identified an erroneous jump in the *Zwally et al.* [2005] results for the AIS. Close examination of Figure 3b of *Zwally et al.* [2005] reveals that the *dh*/*dt* for a region of 100 km radius in the NE AIS for 1992–1996.6 was

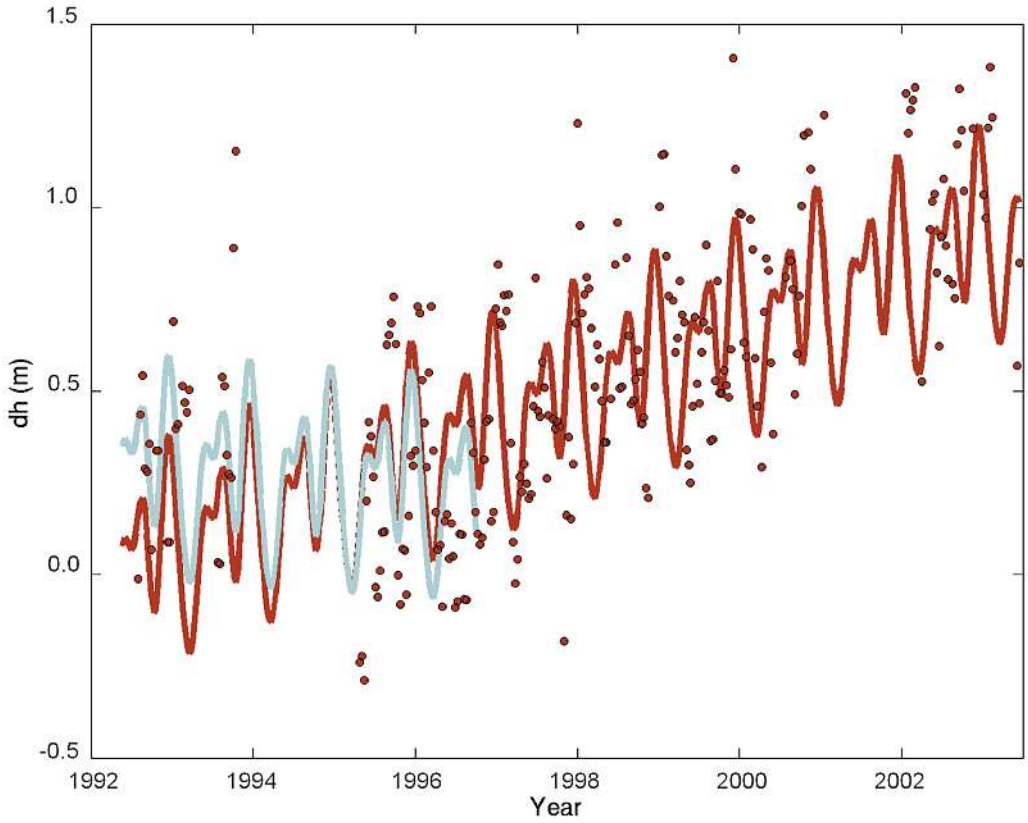

Figure 6. Time series of ERS-ERS elevation using *dh* data from all crossovers within 100 km of the crossover located at 69.64°S, 71.99°E. The red dots are 10-day averages at actual sample epochs. The red and cyan lines are best fitting values (to the unsmoothed data) for the entire and pre-1996.8 periods, respectively. The best fitting model was based on the time series spectra and included a linear term plus periodic terms with one, two, three, and four cycles per year.

-0.001 m a^{-1} (see Figure S1 in the auxiliary material).[1] This was followed by an apparent step in elevation at 1996.6 and subsequent increase in *dh*/*dt* to +0.102 m a^{-1} from 1996.6 to 2001 (giving them a mean rate of +0.15 m a^{-1}). The step is due to an erroneous altimeter bias value at the location of the crossover shown in their Figure 3 and some surrounding points (H. J. Zwally, personal communication, 2007). Correcting for the error (0.46 m) removes the step, leaving a corrected mean *dh*/*dt* for the full period of 0.073 m a^{-1}. Figure 5 may be regarded as a corrected version of their map of *dh*/*dt* for this region.

[35] The mean ERS *dh*/*dt* for the AIS is also shown in Figure 4, both for the entire AIS (filled polygons) and for the region where the GPS and leveling data exist (taking all points north of 72°S). We note that there is little difference between the two mean values, partly due to there being very few ERS *dh*/*dt* estimates in the southernmost section of the AIS.

[36] The GPS-GPS crossovers span a similar period (1995–2003) to the later subset of the ERS record (1996.8–2003). A total of 150 crossovers were available, with mean *dh*/*dt* also shown in Figure 4. The mean *dh*/*dt* is 0.122 m a^{-1} between the 1995 and 2003 surveys and 0.127 m a^{-1} between the 1995 and 2001 surveys. The rate for the shorter period (1999 to 2003) crossovers (0.123 m a^{-1}) is also in close agreement. These are somewhat consistent with the independent ERS rate (0.095 m a^{-1}) over the similar period 1996.8–2003, giving us independent validation of this result. Furthermore, the temporal stability reflected in the various GPS-GPS *dh*/*dt* estimates over the period 1995–2003 is in good agreement with the temporal stability of the ERS-derived *dh*/*dt* for 1996.8–2003 shown in Figure 6. While the error budget of ERS estimates of dh/dt is somewhat complicated by, among others, possible changes in surface characteristics over time [e.g., *Lacroix et al.*, 2007; *Phillips*, 1998], the agreement between independent techniques suggests confidence may be placed in the results. GPS-GPS crossovers covering the period 2003–2006 show a smaller mean *dh*/*dt*, suggesting an ice shelf surface lowering occurs after 2003, at least in the relatively small region sampled by the GPS profiles (Figure 1).

[37] ICESat-ICESat crossovers are analyzed for the period 2003.8–2007.3. The mean *dh*/*dt* crossover values over this most recent period are shown in Figure 7 for the floating AIS and the surrounding grounded ice. On the AIS, a distinct pattern of negative *dh*/*dt* is observed, except

[1] Auxiliary materials are available in the HTML. doi:10.1029/2008JF001094.

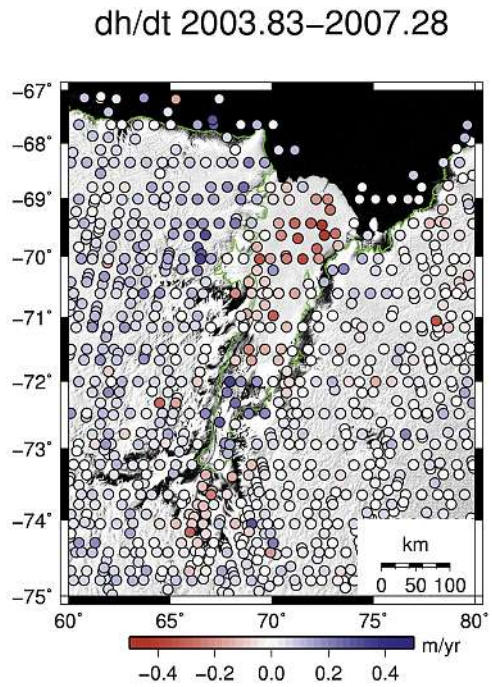

Figure 7. The *dh*/*dt* (2003.83–2007.28) at ICESat-ICESat crossover locations. Data have been filtered as described in the text.

in the southernmost region where there are some strongly positive values. The mean *dh*/*dt* of the entire AIS is −0.119 m a^{-1}; for the region north of 72°S it is −0.184 m a^{-1} (Figure 4). The negative *dh*/*dt* observed in the ICESat crossovers in the region of the GPS data is consistent with the GPS-observed decrease in *dh*/*dt* after 2003 and is also consistent with ENVISAT along-track results (B. Legresy, unpublished data, 2008), showing trends of −0.1 m a^{-1} over the central AIS region (between 70° and 71°S) for the period 2003–2007.

[38] The magnitude of the dominant negative ICESat *dh*/*dt* signal observed is in contrast to the signal on the grounded ice, where small negative values are evident west of the AIS and near-zero values are evident to the east. This is illustrated in the histogram of ICESat-ICESat *dh*/*dt* values (Figure 8). Close examination of the ERS-ERS *dh*/*dt* histograms reveals a similar contrasting relationship between the grounded and floating ice, most notably for the 1996.8–2003 period (Figure 9), although for this data set the pattern is reversed with more positive *dh*/*dt* on the ice shelf than on the grounded ice.

4. Discussion

[39] The net elevation change of the central Amery Ice Shelf over the 39 years from 1968 through 2007 is close to zero and, given the assumed relationship between ice shelf elevation and ice shelf thickness, the central AIS has a near-zero thickness change over this period. Pre-1996.8 ERS trends for the central and northern AIS are consistent with the longer-term net trend along the leveling route. Shifts in ice shelf *dh*/*dt* in mid-1996 and 2003 are each observed in two of the ERS, GPS and ICESat data sets; in both cases the shifts are abrupt. Between 1996.8 and 2003 the ERS-ERS and GPS-GPS crossovers agree that the ice shelf *dh*/*dt* was positive. From 2003, both ICESat-ICESat and GPS-GPS crossovers agree that ice shelf surface *dh*/*dt* decreased, and the ICESat-ICESat crossovers show clear negative *dh*/*dt* after 2003. The GPS-GPS crossovers cover a smaller area more densely than the other techniques, but a consistent pattern is still seen.

[40] Our interpretation of Figure 4 is, therefore, that the central AIS showed a net increase in surface elevation from ~1996.8 to at least 2003, and then began to decrease again. To provide a net near-zero thickness change over the longer record, we interpret the period between 1968 and the early 1990s to have been a period of small net lowering of the central AIS (~−0.01 m a^{-1}), where the lowering is presumably due to an imbalance between local mass budget contributions of accumulation, basal melting, vertical strain thinning and ice thickness advection, and/or variation in firn densification rates. We emphasize that this is an inference of net change and that there may have been periods prior to 1992 where the ice shelf fluctuated as observed in the period after 1996.

[41] Our finding that the central AIS has not undergone substantial net surface elevation change over ~39 years is consistent with the velocity change analysis of *King et al.* [2007] who concluded that the central AIS had undergone only a very small reduction in ice velocity over the period 1968–1999. Simple considerations of force balance in the ice shelf suggest that a regionally slightly thinner ice shelf would be consistent with slightly lower velocities.

[42] Together, the long-term *dh*/*dt* and velocity change data sets provide strong evidence that this region of the AIS remained largely unchanged between 1968 and 2007. Furthermore, they provide baseline measurements against which any future changes of the AIS can be interpreted. Given the ERS-observed thinning of, for example, Larsen B and Wilkins ice shelves that occurred prior to their recent collapses in

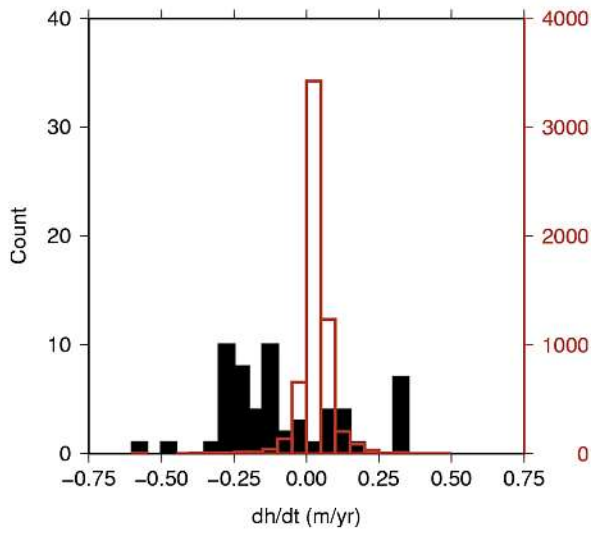

Figure 8. Histogram of *dh*/*dt* measurements shown in Figure 7 from ICESat-ICESat crossovers on the floating AIS (black, left scale) and the grounded ice sheet (red, right scale).

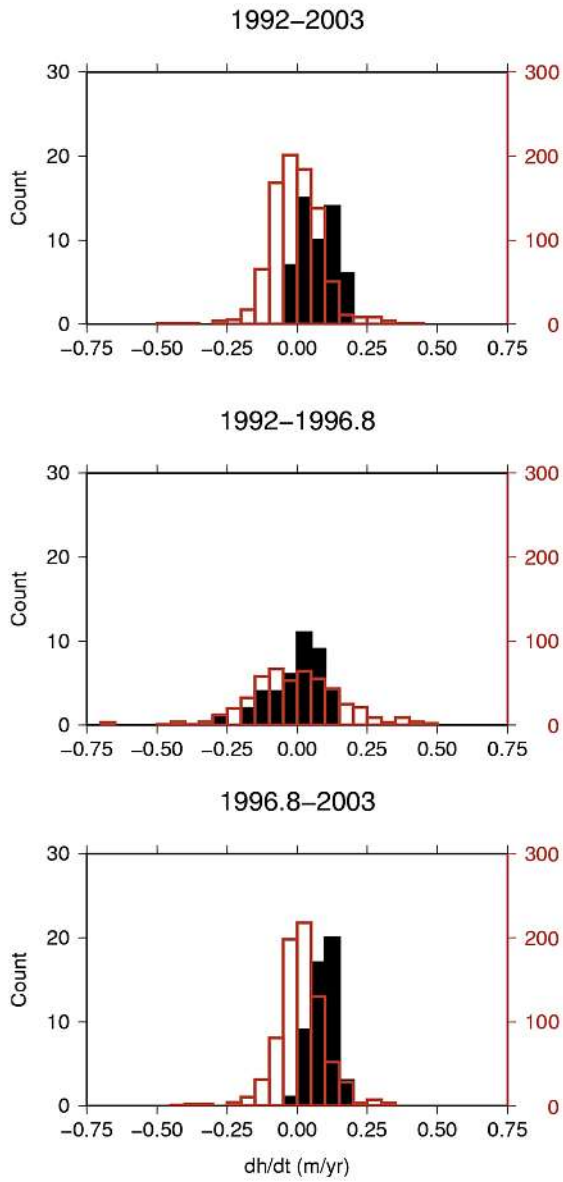

Figure 9. Histogram of *dh*/*dt* measurements shown in Figure 5 from ERS-ERS crossovers on the floating AIS (black, left scale) and the grounded ice sheet (red, right scale).

2002 and 2008 [*Shepherd et al.*, 2003, L. Padman et al., manuscript in preparation, 2008], this is especially important.

[43] Our results also indicate that within short time periods of observation, the AIS has undergone elevation fluctuations of up to ~±0.5 m over 5 years, or up to ±0.1 m a^{-1} (Figure 4). Unfortunately, the GPS-derived velocity data for the AIS do not have sufficiently frequent site reoccupation to determine subdecadal variations which may accompany the observed increase in *dh*/*dt* during 1996 and no GPS-based velocity data are available over the 2003 period. SAR-derived velocity data are also sparse during this time frame.

[44] There are several potential contributors to the observed interdecadal fluctuations in surface elevation: (1) surface mass balance; (2) firn densification; and (3) basal processes. We examine each of these in turn below.

[45] 1. Surface mass balance: *Budd et al.* [1982] give values of 1962–70 mean snow accumulation rate, ranging from 1.2 m a^{-1} (~0.45 m a^{-1} water equivalent (w.e.)) at the ice shelf front to 0.42 m a^{-1} (~0.16 m a^{-1} w.e.) at the southern extent of our observation network. Combining these observations with considerations of the buoyancy of the ice shelf using an ocean water density of 1028 kg m^{-3}, in agreement with *Fricker et al.* [2001], and the implied densities of snow from above, translates to an influence on ice shelf elevation from 0.26 m a^{-1} (southern extent of our network) to 0.76 m a^{-1} (northern extent). If the ice shelf is in steady state, this accumulated mass is balanced by thinning, basal melt/freeze and thickness advection, with the snowpack densifying to firn and ice to maintain an average surface elevation. The annual periodic variations in Figure 6 indicate that there are regular seasonal aspects to this balance, although this could also be related to seasonal altimeter measurement bias. Clearly if an individual year has annual accumulation that is substantially different to the average there would be a corresponding anomaly in elevation. This could influence inferred rates of elevation change that are only based on initial and final measurements, rather than continuous monitoring.

[46] *Monaghan et al.* [2006] modeled decadal level accumulation variations compared to regional means over the period 1955–2004 using ice core records and the ERA-40 meteorological reanalysis. From their Figure 2 (and assuming regional coherence in long-term accumulation rates) we infer that the region around the AIS experienced about 5% reduction in accumulation over the period 1955–1995 followed by about 15% increase in accumulation over the period 1995–2004. Converting these to ice shelf elevation change anomalies relative to the long-term mean snowfall rates of *Budd et al.* [1982] (as given above) would yield values between −0.01 and −0.04 m a^{-1} (1968–1995) and between +0.04 m a^{-1} and +0.11 m a^{-1} (1995–2004). These variations would match the signs and be close to the magnitude of the measured *dh*/*dt* of −0.01 m a^{-1} (1968–1996) and +0.10 m a^{-1} (1996–2003), but such an analysis ignores the matter of firn densification. Over years and decades, these accumulation anomalies will result in variations in densification rate [e.g., *Arthern and Wingham*, 1998] and hence we regard this agreement as probably being fortuitous; densification issues are discussed below.

[47] Furthermore, the observed elevation changes on the ice shelf during 1996–2007 are anomalously large when compared to those on the surrounding grounded ice, further suggesting that decadal accumulation variations, which have larger spatial scales that that of the AIS [*Monaghan et al.*, 2006], are not directly responsible. For example, Figure 7 shows that the recent negative *dh*/*dt* of the Northern AIS is of opposite sign to the surrounding *dh*/*dt* signal over the grounded ice sheet. We therefore consider that accumulation variations are unable to account for the recent fluctuations in AIS elevation revealed by our analysis.

[48] 2. Firn densification: We did not correct for the effects of varying firn densification on the observed *dh*/*dt*. Densification rates are sensitive to both temperature and accumulation fluctuations [*Arthern and Wingham*, 1998; *Helsen et al.*, 2008; *Zwally and Li*, 2002], and since they do not reflect mass change, they bias estimates of ice shelf mass balance derived from *dh*/*dt*. Previous altimeter-based

studies of Antarctic *dh*/*dt* generally did not model this effect, or applied only a temperature-based model [*Zwally et al.*, 2005]; see also the review of *Alley et al.* [2007] and references therein. The magnitude of the *Zwally et al.* [2005] modeled temperature-driven effect is generally small in East Antarctica, being $\sim$+0.002 m a^{-1} on average, and no more than $\sim\pm$0.01 m a^{-1} for the AIS [*Zwally et al.*, 2005, Figure 9]. Recently, however, *Helsen et al.* [2008] have reported on a model of the effect of accumulation anomalies on measured *dh*/*dt* and suggested that substantial biases may exist if the effect is not corrected. In particular they find that *dh*/*dt* can depend on both current and decadal to multidecadal average accumulation rates. For the 1995–2003 ERS-2 period, they report an effect on measured *dh*/*dt* incorporating anomalies in the depth of the firn layer that reaches ± 0.2 m a^{-1}. Their estimates of the effect for the AIS are between approximately +0.02 and +0.08 m a^{-1} (estimated from *Helsen et al.* [2008, Figure 2a]) for 1995–2003. This densification anomaly would somewhat explain our observed 1996–2003 *dh*/*dt*, although it remains to be seen whether the model also agrees with the earlier or later observations. However, *Helsen et al.* [2008, Figure S9g] also show that their 1995–2003 estimate for the AIS is not statistically different from zero at the 2σ level, mainly due to large uncertainty in their 25-year accumulation trend for this region (their Figure S9e). Furthermore, it does not agree with our observations that the AIS *dh*/*dt* during 1996.8–2003 and 2003–2007 are anomalous compared to the surrounding grounded ice, since their modeled correction is continuous across the grounding zone [*Zwally et al.*, 2005, Figure 2a]. It may be that this is a result of their limited model resolution and that a focused AIS-based study into firn densification would improve their presently uncertain estimates. Passive microwave data have been used to infer AIS ice melt extent and intensity over the period 1978–2003 [*Liu et al.*, 2006] and these suggest that melt in the region of the AIS is almost exclusively confined to the ice shelf, offering the possibility that the observed elevation changes are related to surface melt. However, the time series of *Liu et al.* [2006] shows no obvious signal that could be related to the mid-1990s elevation increase we observe. In contrast, around the time of the observed elevation decrease a positive melt anomaly (relative to the slightly decreasing trend) does occur in austral summer 2002–3, in general agreement with AWS temperatures that show January temperatures in 2003–2006 to be positive anomalies to the long-term trend (I. Allison, personal communication, 2008). Further ice core, AWS, remote sensing and model studies are required to further explore the impact of firn densification on our data sets.

[49] On longer time scales, *Helsen et al.* [2008] suggest that *dh* biases due to firn densification alone could theoretically reach as high as 1 m over 50 years, or 0.02 m a^{-1}, although the value for the AIS on these time scales is at present completely uncertain. Until improved longer-term model results are available, based on local ice cores, this possible uncertainty should be considered alongside our stated uncertainty estimates for our long *dh*/*dt* record. The meteorological modeling of *Helsen et al.* [2008] does predict increased snowfall and warmer temperatures over the AIS during 1995–2003 (their Figures S5a and S5c). Importantly, the relative effect on ERS-derived *dh*/*dt* of variability in firn densification, compared to that of the other techniques is not known, but is likely to be different owing to the possible effect of changing subsurface reflectors on radar altimetry [*Thomas et al.*, 2008].

[50] 3. Basal processes: Ice-ocean modeling suggests that the central AIS is dominated by regions of net basal melt of between zero and 1.0 m a^{-1} of ice [*Williams et al.*, 2002], representing a present-day contribution to elevation reduction of 0.00–0.10 m a^{-1}. There is little direct observational oceanographic data from this region to constrain ocean temperature and circulation changes over the relevant time scales. However, preliminary regional oceanographic model runs show that changes in ocean temperature can affect basal melt rates on suitable magnitudes (B. Galton-Fenzi, personal communication, 2008). The spatial and temporal pattern of the related surface elevation change requires further exploration with more sophisticated model runs. Furthermore, the ocean circulation effects of a major calving event around 1963 [*Fricker et al.*, 2002] and subsequent advance of the ice front also remain to be explored by computer modeling.

[51] In addition to these three effects, small-scale topographic features on the ice shelf are advected downstream with the net ice flow, with typical velocities on the AIS being 300–1300 m a^{-1}. As discussed above, the effect of this on the longer-term data set is <-0.01 m a^{-1} in terms of a systematic bias. For the shorter periods, we performed further Monte Carlo simulations and found that biases due to advection may exist in our mean GPS–GPS *dh*/*dt* with magnitudes $<\pm$0.01 m a^{-1}. The ERS and ICESat crossovers cover longer periods and larger regions than the GPS-GPS crossovers, and hence this value represents an upper bound to the topography-related mean *dh*/*dt* in those records.

[52] After considering these potential contributions to the observed changes in *dh*/*dt*, we are still uncertain as to their cause. They must, therefore, be due to changes in some currently poorly understood process (either ice dynamics, or basal mass exchange) or poorly quantified firn column changes.

5. Conclusions

[53] We have analyzed a 4-decade record (1968–2007) of surface height data for the central Amery Ice Shelf and found that its elevation (and hence thickness) remained largely unchanged in net terms over this period. It was essential to exploit recent advances in geoid, mean dynamic ocean topography and tide models to avoid large biases in *dh*/*dt* based on the 1968 leveling data that we reanalyzed from raw field notes. This data set now represents one of the longest and best observed records of height change of a large Antarctic ice shelf and provides baseline data against which shorter period fluctuations must be interpreted.

[54] In contrast to the longer record, the *dh*/*dt* values computed during the period of continuous observation are complex; the AIS elevation apparently deviated from its mean by 0.5–1.0 m over two periods of less than 7 years. The speed at which the ice shelf *dh*/*dt* changes is surprising and suggests caution should be exercised in interpreting ice shelf surface height trends. *Zwally et al.* [2005] identify

many ice shelves with strong *dh*/*dt* signals, but the record we present here suggests that it is possible that these trends may change in the future without necessarily signaling ice shelf instability. Insufficient observations on the AIS in the 1968–1992 period mean that only the net elevation change is measured and the fluctuations after near-continuous observations began in 1992 cannot be regarded as unique to this latter period. The dominant source(s) of these variations are not yet known and further investigation is required, especially in relation to the observed changes in *dh*/*dt* in mid-1996 and 2003. We consider that the observed changes are not caused by accumulation fluctuations. This leaves presently unidentified changes in ice shelf dynamics, basal or subshelf processes, or presently poorly quantified firn processes (including those related to surface melt) or basal melt variations as the foci for future observational and model-based investigations.

[55] Our results highlight the importance of continuous, multidecadal observations of ice shelf elevation and show that interpretation of elevation changes spanning short time periods can be misleading especially when seeking to extrapolate results beyond the observation interval.

[56] **Acknowledgments.** We thank Jo Jacka, Andrew Ruddell, and Neal Young for assistance in accessing the 1968 field notes and Max Corry for help in interpreting them. We thank NASAs ICESat Science Project and the NSIDC for distribution of the ICESat data, see http://icesat.gsfc.nasa.gov and http://nsidc.org/data/icesat. ERS radar altimeter data is copyrighted to the ESA and was provided by Jay Zwally at the Cryospheric Sciences Branch of the Hydrospheric and Biospheric Sciences Laboratory of NASA/GSFC, with special thanks to Jairo Santana and Helen Cornejo. Additional data sets were kindly provided by Ian Barnes-Keoghan of the Australian Bureau of Meteorology (atmospheric pressure), Ian Allison (AWS data), Don Chambers (raw DOT), and Chris Watson (Davis sea level analysis). Dave McAdoo clarified the permanent tide system of ICESat and relevant corrections. Review comments by Reinhard Dietrich, two other anonymous reviewers, and Martin Truffer (AE) were helpful in improving the paper. The efforts of the various field parties are gratefully acknowledged. GPS field data collection was supported by Australian ASAC and ARC grants held by RC. A.F. and M.A.K. were supported by NERC (UK) grant NE/C000862/1 and M.A.K. was also supported by an NERC fellowship. H.A.F. and L.P. were supported by NASA grant NNG05GR58G. This work was partly supported by the Australian Governments Cooperative Research Centre Programme through the Antarctic Climate and Ecosystem CRC. This is ESR contribution 99.

References

Alley, R. B., M. K. Spencer, and S. Anandakrishnan (2007), Ice-sheet mass balance: Assessment, attribution and prognosis, *Ann. Glaciol.*, *46*, 1–7, doi:10.3189/172756407782871738.

Altamimi, Z., P. Sillard, and C. Boucher (2002), ITRF2000: A new release of the International Terrestrial Reference Frame for earth science applications, *J. Geophys. Res.*, *107*(B10), 2214, doi:10.1029/2001JB000561.

Arthern, R. J., and D. J. Wingham (1998), The natural fluctuations of firn densification and their effect on the geodetic determination of ice sheet mass balance, *Clim. Change*, *40*, 605–624, doi:10.1023/A:1005320713306.

Blewitt, G., and D. Lavallée (2002), Effect of annual signals on geodetic velocity, *J. Geophys. Res.*, *107*(B7), 2145, doi:10.1029/2001JB000570.

Budd, W. F., M. J. Corry, and T. H. Jacka (1982), Results from the Amery Ice Shelf Project, *Ann. Glaciol.*, *3*, 36–41.

Chambers, D. P. (2006), Observing seasonal steric sea level variations with GRACE and satellite altimetry, *J. Geophys. Res.*, *111*, C03010, doi:10.1029/2005JC002914.

Chen, G. (1998), GPS kinematic positioning for the airborne laser altimetry at Long Valley, California, Ph.D. thesis, 173 pp., Mass. Inst. of Technol., Cambridge, Mass.

Dorrer, E., W. Hofmann, and W. Seufert (1969), Geodetic results of the Ross Ice Shelf Survey expeditions, 1962–63 and 1965–66, *J. Glaciol.*, *8*, 67–90.

Egbert, G. D., and S. Y. Erofeeva (2002), Efficient inverse modeling of barotropic ocean tides, *J. Atmos. Oceanic Technol.*, *19*, 183–204, doi:10.1175/1520-0426(2002)019<0183:EIMOBO>2.0.CO;2.

Femenias, P. (1996), ERS QLOPR and OPR range processing, *ESA/ESRIN Tech. Note ER-TN-RS-RA-0022*, Eur. Space Agency/Eur. Space Res. Inst., Frascati, Italy.

Förste, C., et al. (2008), The GeoForschungsZentrum Potsdam/Groupe de Recherche de Gèodésie Spatiale satellite-only and combined gravity field models: EIGEN-GL04S1 and EIGEN-GL04C, *J. Geod.*, *82*, 331–346, doi:10.1007/s00190-007-0183-8.

Fricker, H. A., S. Popov, I. Allison, and N. Young (2001), Distribution of marine ice beneath the Amery Ice Shelf, *Geophys. Res. Lett.*, *28*, 2241–2244, doi:10.1029/2000GL012461.

Fricker, H. A., N. W. Young, I. Allison, and R. Coleman (2002), Iceberg calving from the Amery Ice Shelf, East Antarctica, *Ann. Glaciol.*, *34*, 241–246, doi:10.3189/172756402781817581.

Fricker, H. A., A. Borsa, B. Minster, C. Carabajal, K. Quinn, and B. Bills (2005), Assessment of ICESat performance at the Salar de Uyuni, Bolivia, *Geophys. Res. Lett.*, *32*, L21S06, doi:10.1029/2005GL023423.

Heil, P. (2006), Atmospheric conditions and fast ice at Davis, East Antarctica: A case study, *J. Geophys. Res.*, *111*, C05009, doi:10.1029/2005JC002904.

Helsen, M. M., M. R. van den Broeke, R. S. W. van de Wal, W. J. van de Berg, E. van Meijgaard, C. H. Davis, Y. Li, and I. Goodwin (2008), Elevation changes in Antarctica mainly determined by accumulation variability, *Science*, *320*, 1626–1629, doi:10.1126/science.1153894.

Ivins, E. R., and T. S. James (2005), Antarctic glacial isostatic adjustment: A new assessment, *Antarct. Science*, *17*, 541–553, doi:10.1017/S0954102005002968.

Kalnay, E., et al. (1996), The NCEP/NCAR 40-year reanalysis project, *Bull. Am. Meteorol. Soc.*, *77*, 437–471, doi:10.1175/1520-0477(1996)077<0437:TNYRP>2.0.CO;2.

King, M., and S. Aoki (2003), Tidal observations on floating ice using a single GPS receiver, *Geophys. Res. Lett.*, *30*(3), 1138, doi:10.1029/2002GL016182.

King, M. A., and L. Padman (2005), Accuracy assessment of ocean tide models around Antarctica, *Geophys. Res. Lett.*, *32*, L23608, doi:10.1029/2005GL023901.

King, M. A., N. T. Penna, P. J. Clarke, and E. C. King (2005), Validation of ocean tide models around Antarctica using onshore GPS and gravity data, *J. Geophys. Res.*, *110*, B08401, doi:10.1029/2004JB003390.

King, M. A., R. Coleman, P. J. Morgan, and R. S. Hurd (2007), Velocity change of the Amery Ice Shelf, East Antarctica, during the period 1968–1999, *J. Geophys. Res.*, *112*, F01013, doi:10.1029/2006JF000609.

King, R. W., and Y. Bock (2006), *Documentation for the GAMIT GPS Analysis Software*, *version 10.3*, Mass. Inst. of Technol., Cambridge, Mass.

Lacroix, P., B. Legresy, R. Coleman, M. Dechambre, and F. Remy (2007), Dual-frequency altimeter signal from Envisat on the Amery Ice Shelf, *Remote Sens. Environ.*, *109*, 285–294, doi:10.1016/j.rse.2007.01.007.

Liu, H. X., L. Wang, and K. C. Jezek (2006), Spatiotemporal variations of snowmelt in Antarctica derived from satellite scanning multichannel microwave radiometer and Special Sensor Microwave Imager data (1978–2004), *J. Geophys. Res.*, *111*, F01003, doi:10.1029/2005JF000318.

McCarthy, D. D., and G. Petit (2004), IERS conventions (2003), *IERS Tech. Note 32*, 127 pp., Bundesamts für Kartographie und Geodäsie, Frankfurt, Germany.

Monaghan, A. J., et al. (2006), Insignificant change in antarctic snowfall since the international geophysical year, *Science*, *313*, 827–831, doi:10.1126/science.1128243.

Padman, L., M. King, D. Goring, H. Corr, and R. Coleman (2003), Ice shelf elevation changes due to atmospheric pressure variations, *J. Glaciol.*, *49*, 521–526, doi:10.3189/172756503781830386.

Phillips, H. A. (1998), Surface meltstreams on the Amery Ice Shelf, East Antarctica, *Ann. Glaciol.*, *27*, 177–181.

Rignot, E., G. Casassa, P. Gogineni, W. Krabill, A. Rivera, and R. Thomas (2004), Accelerated ice discharge from the Antarctic Peninsula following the collapse of Larsen B ice shelf, *Geophys. Res. Lett.*, *31*, L18401, doi:10.1029/2004GL020697.

Scambos, T., C. Hulbe, M. Fahnestock, and J. Bohlander (2000), The link between climate warming and break-up of ice shelves in the Antarctic Peninsula, *J. Glaciol.*, *46*, 516–530, doi:10.3189/172756500781833043.

Scharroo, R., and P. Visser (1998), Precise orbit determination and gravity field improvement for the ERS satellites, *J. Geophys. Res.*, *103*, 8113–8127, doi:10.1029/97JC03179.

Scheinert, M., J. Müller, R. Dietrich, D. Damaske, and V. Damm (2008), Regional geoid determination in Antarctica utilizing airborne gravity and topography data, *J. Geod.*, *82*, 403–414, doi:10.1007/s00190-007-0189-2.

Schofield, W. (1993), *Engineering Surveying*, 4th ed., 554 pp., Butterworth-Heinemann, Oxford, U. K.

Schutz, B. E., H. J. Zwally, C. A. Shuman, D. Hancock, and J. P. DiMarzio (2005), Overview of the ICESat Mission, *Geophys. Res. Lett.*, *32*, L21S01, doi:10.1029/2005GL024009.

Shepherd, A., D. Wingham, T. Payne, and P. Skvarca (2003), Larsen ice shelf has progressively thinned, *Science*, *302*, 856–859, doi:10.1126/science.1089768.

Shuman, C. A., H. J. Zwally, B. E. Schutz, A. C. Brenner, J. P. DiMarzio, V. P. Suchdeo, and H. A. Fricker (2006), ICESat Antarctic elevation data: Preliminary precision and accuracy assessment, *Geophys. Res. Lett.*, *33*, L07501, doi:10.1029/2005GL025227.

Thomas, R., C. Davis, E. Frederick, W. Krabill, Y. Li, S. Manizade, and C. Martin (2008), A comparison of Greenland ice-sheet volume changes derived from altimetry measurements, *J. Glaciol.*, *54*, 203–212, doi:10.3189/002214308784886225.

Watson, C. S. (2005), Satellite altimeter calibration and validation using GPS buoy technology, Ph.D. thesis, 264 pp., Univ. of Tasmania, Hobart, Australia.

Wessel, P., and W. H. F. Smith (1998), New, improved version of generic mapping tools released, *Eos Trans. AGU*, *79*(47), 579, doi:10.1029/98EO00426.

Williams, M. J. M., R. C. Warner, and W. F. Budd (2002), Sensitivity of the Amery Ice Shelf, Antarctica, to changes in the climate of the Southern Ocean, *J. Clim.*, *15*, 2740–2757, doi:10.1175/1520-0442(2002)015<2740:SOTAIS>2.0.CO;2.

Zwally, H. J., and A. C. Brenner (2001), Ice sheet dynamics and mass balance, in *Satellite Altimetry and Earth Science*, edited by L.-L. Fu and A. Cazenave, pp. 351–369, Academic, San Diego, Calif.

Zwally, H. J., and J. Li (2002), Seasonal and interannual variations of firn densification and ice-sheet surface elevation at the Greenland summit, *J. Glaciol.*, *48*, 199–207, doi:10.3189/172756502781831403.

Zwally, H. J., M. B. Giovinetto, J. Li, H. G. Cornejo, M. A. Beckley, A. C. Brenner, J. L. Saba, and D. Yi (2005), Mass changes of the Greenland and Antarctic ice sheets and shelves and contributions to sea-level rise: 1992–2002, *J. Glaciol.*, *51*, 509–527, doi:10.3189/172756505781829007.

R. Coleman, Centre for Marine Science, University of Tasmania, Private Bag 78, Hobart, Tasmania 7001, Australia.

A.-J. Freemantle and M. A. King, School of Civil Engineering and Geosciences, Newcastle University, Newcastle upon Tyne NE1 7RU, UK. (m.a.king@newcastle.ac.uk)

H. A. Fricker, Institute of Geophysics and Planetary Physics, Scripps Institution of Oceanography, La Jolla, CA 92093, USA.

R. S. Hurd, Center for Spatial Information Science, University of Tasmania, Private Bag 76, Hobart, Tasmania 7001, Australia.

B. Legrésy, LEGOS, CNES, UPS, IRD, CNRS, 14 avenue Edouard Belin, Toulouse, F-31400, France.

L. Padman, Earth and Space Research, 3350 SW Cascade Avenue, Corvallis, OR 97333-1536, USA.

R. Warner, Australian Antarctic Division, Department of the Environment, Water, Heritage, and the Arts, Channel Highway, Kingston, Tasmania 7050, Australia.